

## Influence of thermochemical treatments on TSMG YBCO bulks doped with Li and Al

This article has been downloaded from IOPscience. Please scroll down to see the full text article.

2010 J. Phys.: Conf. Ser. 234 012011

(<http://iopscience.iop.org/1742-6596/234/1/012011>)

View [the table of contents for this issue](#), or go to the [journal homepage](#) for more

Download details:

IP Address: 128.131.38.71

The article was downloaded on 10/08/2010 at 10:22

Please note that [terms and conditions apply](#).

# Influence of thermochemical treatments on TSMG YBCO bulks doped with Li and Al.

P. Diko<sup>1</sup>, V. Antal<sup>1</sup>, M. Kaňuchová<sup>1</sup>, M. Šefčíková<sup>1</sup>, J. Kováč<sup>1</sup>, X. Chaud<sup>2</sup>,  
M Eisterer<sup>3</sup>, N. Hörhager<sup>3</sup>, M. Zehetmayer<sup>3</sup>, H. W. Weber<sup>3</sup>

<sup>1</sup> Institute of Experimental Physics SAS, Watsonova 47, 04001 Košice, Slovakia

<sup>2</sup> CNRS/CRETA, 25, Avenue des Martyrs, 38042 Grenoble Cedex 9, France

<sup>3</sup> Vienna University of Technology, Atominstitut, Stadionallee 2, 1020 Vienna, Austria

E-mail: [dikos@saske.sk](mailto:dikos@saske.sk)

**Abstract.** The influence of post-growth thermochemical treatments on the transition temperature and the field dependence of the critical current density at 77 K were studied in  $Y_{1.5}Ba_2(Cu,M)_3O_y$ , for  $M = Li$ , and Al, bulk superconductors with  $CeO_2$  additions prepared by the Top-Seeded Melt-Growth (TSMG) process. The Li and Al dopants react in an opposite way during pre-annealing in an atmosphere with low and high oxygen partial pressure and this behaviour can be associated with the formation and dissolution of dopant clusters. High pressure high temperature oxygenation preserves the peak effect introduced by the dopants and leads to the elimination of oxygenation cracks and consequently to significant increases in the effective critical current density.

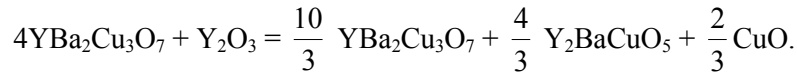
## 1. Introduction

As a consequence of the small coherence length ( $\approx 3$  nm at 77 K), the most effective pinning centers in RE123 superconductors should have nanosize dimensions. Successful attempts to introduce nanosize pinning centers in the form of chemical substitutions in the RE123 lattice were reported [1, 2]. It is characteristic for TSMG RE123, especially for Y123, that small additions of Pt or Ce are necessary for their successful fabrication. These elements may react with the added substitutions and consequently misrepresent their influence on the pinning behavior. All reported studies on TSMG YBCO bulks with Cu substitutions were done on systems with Pt additions, which could be the reason why chemical pinning by some dopants, substituting Cu in the Y123 lattice, has not been observed in YBCO bulk superconductors so far. For example in the TSMG Y123 bulks with Pt addition the  $(Ba_3Y)Al_2PtO_x$  type phase is formed, which can incorporate some Cu substituents [3]. Therefore, in the present study of TSMG YBCO bulks the  $CeO_2$  additions were used.

As-grown  $YBa_2Cu_3O_7$  bulk superconductors have a low oxygen content,  $YBa_2Cu_3O_{6.3}$ , are not superconducting and must be oxygenated to  $YBa_2Cu_3O_7$ . In this contribution we present the influence of three different post-growth heat treatments, pre-annealing in oxygen or argon atmosphere followed by standard oxygenation at 400 °C and high pressure high temperature oxygenation, on the transition temperature,  $T_c$ , and the critical current density,  $J_c$ , in Li or Al doped YBCO bulk samples.

## 2. Experimental details

Doped YBCO bulk single – grain superconductors were fabricated by the TSMG process in a chamber furnace using Sm123 seeds. Powders  $YBa_2Cu_3O_7$ ,  $Y_2O_3$ ,  $Al_2O_3$ , or  $Li_2CO_3$  and  $CeO_2$  (0.5 wt.%) [3] for processing reactions were milled for 20 minutes in a friction mill and pressed into cylindrical pellets of 20 mm in diameter with a thickness of 12 mm. The dopants were added in amounts to reach the chosen dopant M (Li or Al) concentration in the  $YBa_2(Cu_{1-x}M_x)_3O_7$  phases after reaction:



Five different M concentrations  $x$  were used for substitution:  $x = 0.0025, 0.005, 0.001, 0.02$  and  $0.05$ . Undoped YBCO was made as a reference for comparison with the M – doped samples.

Small samples for oxygenation and magnetization measurements were cut from the  $a$  – growth sector of the top surface of the bulks at a distance of 1 mm from the seed. The samples had the shape of a slab with dimensions of  $2 \times 2 \times 0.5 \text{ mm}^3$ , the smallest dimension was parallel to the  $c$  – axis of the crystal.

Three different post-growth thermochemical heat treatments were applied on the small separated samples:

- annealing in oxygen flow in a tubular furnace at  $800 \text{ }^\circ\text{C}$  for 2 hours, slow cooling to  $400 \text{ }^\circ\text{C}$ , oxygenation there for 240 hours, and finally slow cooling to room temperature (referred to as standard oxygenation, SO).
- annealing in argon flow at  $800 \text{ }^\circ\text{C}$  for 2 hours, slow cooling to  $400 \text{ }^\circ\text{C}$  in argon, oxygenation in oxygen flow at  $400 \text{ }^\circ\text{C}$  for 240 hours, slow cooling to room temperature (referred to as Argon).
- high pressure, high temperature oxygenation at  $750 \text{ }^\circ\text{C}$  (referred as HPO, details described in [4])

The magnetization measurements were done at a temperature of  $77 \text{ K}$  in a vibrating – sample magnetometer in magnetic fields of up to  $5 \text{ T}$  applied parallel to the  $c$  – axis of the crystal. The critical current density,  $J_c$ , was calculated from magnetization hysteresis loops using the modified Bean model [5]. The transition temperatures,  $T_c$ , were determined from the magnetic transition curves taken after zero – field cooling as the mid – point of these curves in an applied external magnetic field of  $2 \text{ mT}$ .

### 3. Results

#### *Microstructure*

The typical microstructure of the as-grown samples observed on the  $a/c$ -surface is shown in Figure 2. The microstructure analysis of all doped samples demonstrated that the Li or Al additions do not form any compound with Y, Ba, Cu or Ce in the system; therefore, we assume that the dopants are diluted in the system. The Y211 particles typically have a bimodal distribution, observed in the samples prepared with  $\text{Y}_2\text{O}_3$  additions combined with friction milling [6], and the Y211 particle size is not significantly refined by  $\text{CeO}_2$  additions, being  $1.4 \text{ } \mu\text{m}$  for undoped samples. This quite large 211 particle size explains why the basic level of the critical current density at  $77 \text{ K}$  is not very high.

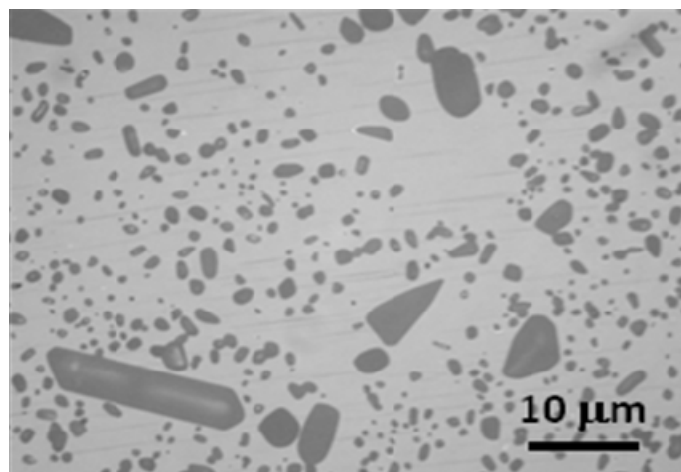


Figure 1. Typical microstructure of as-grown samples with bimodal size distribution of Y211 particles in the single crystalline Y123 matrix.

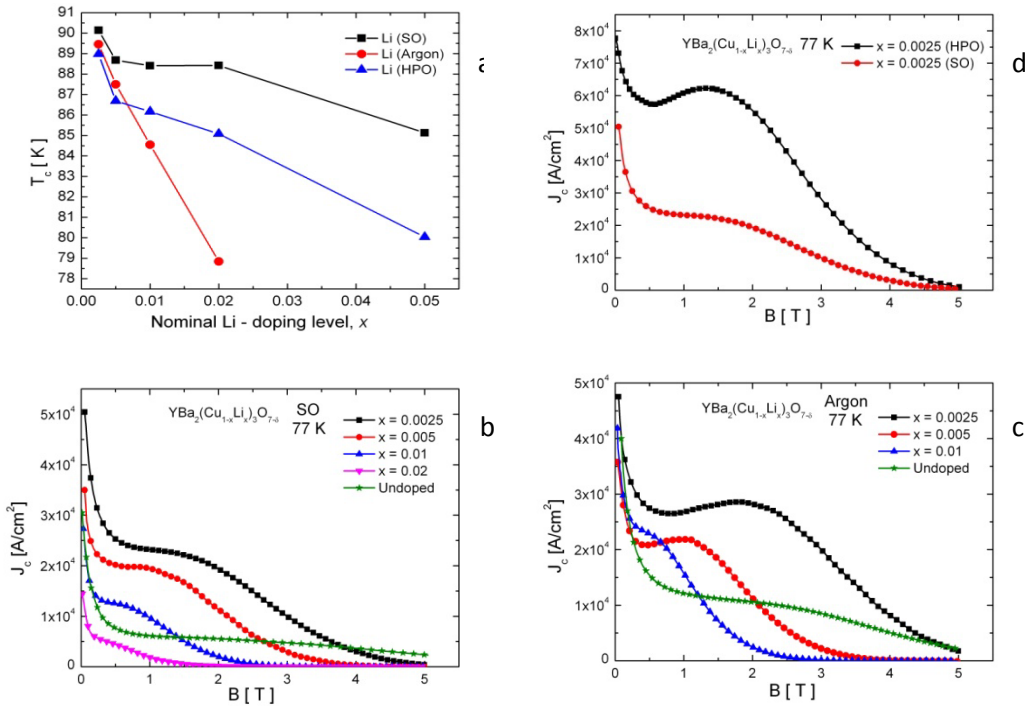


Figure 2. Influence of post-growth thermochemical treatments of  $\text{YBa}_2(\text{Cu}_{1-x}\text{Li}_x)_3\text{O}_7$  bulks on the transition temperature  $T_c$  (a) and field dependence of the critical current density (b) – (d) at 77 K.

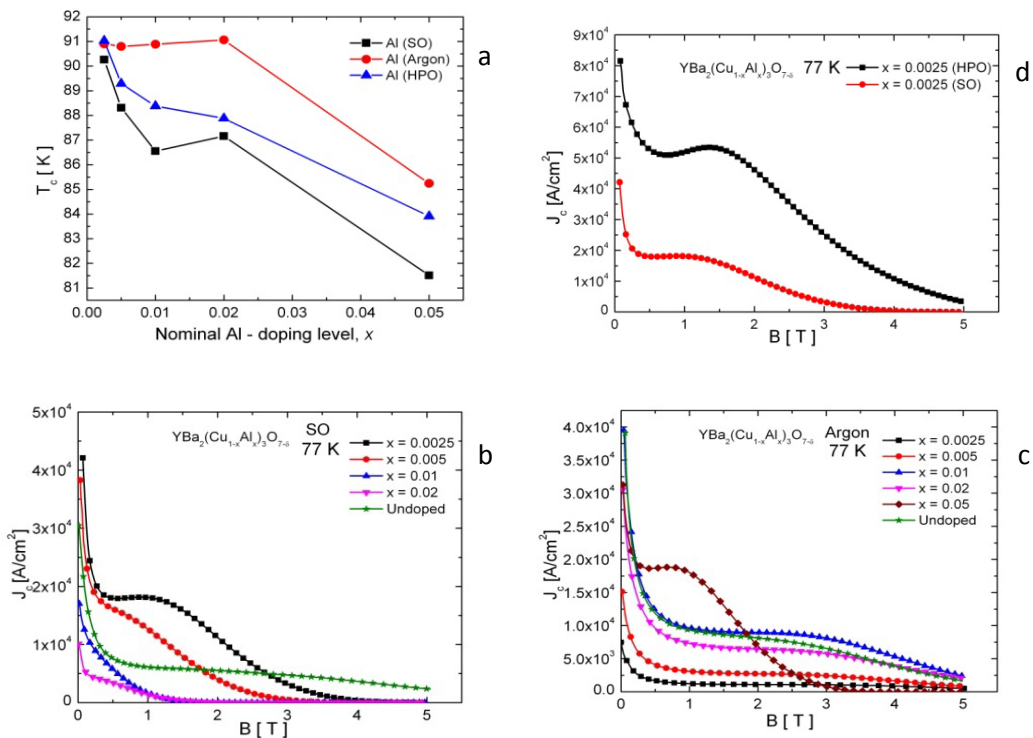


Figure 3. Influence of post-growth thermochemical treatments of  $\text{YBa}_2(\text{Cu}_{1-x}\text{Al}_x)_3\text{O}_7$  bulks on the transition temperature  $T_c$  (a) and field dependence of the critical current density (b) – (d) at 77 K.

#### *Influence of dopants and oxygenation on $J_c$ and $T_c$*

The decrease of the transition temperature by Li doping was, besides the Li concentration, significantly influenced by the type of post-growth heat treatment (Figure 2 (a)). Standard oxygenation suppressed  $T_c$  only mildly.  $T_c$  was strongly suppressed by high pressure oxygenation and the most harmful influence on  $T_c$  was pre-annealing in Ar at 800 °C. A peak effect in the dependence of the measured critical current density on the applied magnetic field at 77 K was observed for the lowest dopant concentration,  $x = 0.0025$  (Figure 2(b)). Pre-annealing in Ar caused a much more pronounced peak effect, mainly in the sample with  $x = 0.0025$  (Figure 2 (c)). The absolute value of the critical current density significantly improved after high pressure oxygenation (Figure 2 (d)).

The applied post-growth heat treatment influenced the  $T_c$  decrease by Al doping in the opposite way than in the previous case (Figure 3 (a)). The sharpest  $T_c$  decrease was observed for the Al doped samples after standard oxygenation. High pressure oxygenation led to a mild increase of  $T_c$  at all Al concentrations. Pre-annealing in Ar did not change  $T_c$  up to an Al concentration  $x = 0.02$  and only then led to a decrease at the Al concentration  $x = 0.05$ . The most pronounced peak effect was observed at an Al concentration of 0.0025 for standard oxygenation and for high pressure oxygenation (Figure 3 (b) and (d)). In samples pre-annealed in Ar, the peak effect was shifted to the highest Al concentration  $x = 0.05$  (Figure 3 (c)). The critical current density was about 2.5 times higher after high pressure oxygenation (Figure 3 (d)) than after standard oxygenation or pre-annealing in Ar.

#### **4. Discussion**

The most obvious difference between Li and Al doped samples is the influence of the post-growth heat treatments on  $T_c$ . Pre-annealing in argon causes a sharp drop of  $T_c$  with Li concentration, while for Al doping  $T_c$  remains constant up to  $x = 0.2$ . Al substitutes for Cu in the CuO chains of the Y123 lattice [7] and should behave similarly to Fe and Co substitutions. Both of these elements with a valence 3+ favour a coordination number,  $n_k$ , higher than 2, and therefore, after annealing in Ar at higher temperatures they share deficient oxygen atoms and form clusters [8]. If Al is concentrated in clusters, the Y123 matrix remains free of Al, with the same  $T_c$  as the undoped sample. We propose that only at an Al concentration  $x = 0.05$  the Al clusters get so close to each other that they influence  $T_c$  of the system. The observed mild increase of  $T_c$  in Al doped samples after high pressure oxygenation may indicate a lower oxygen content in the Y123 matrix after this treatment and therefore some Al clustering.

On the other hand the valence state of the Li ion in Y123 can be considered to be monovalent. Opinions where Li goes are controversial. While Nicolas - Francillona et al., Liu et al. and Kwei et al. [9-11] proposed substitution of Cu in the Cu-O chains, Maury et al. [12] proposed a total substitution in the  $\text{CuO}_2$  planes (orthorhombic Y123) or a partial substitution in the Cu-O chains (tetragonal Y123). If we assume that Li substitutes Cu in Cu-O chains with  $n_k = 2$ , similar to Ag [13], it is possible to draw the following scenario for the Li redistribution due to the post-growth thermochemical treatments. In Figure 4, various oxygen configurations about the metal atom in the  $\text{CuO}_2$  plane are shown [14]. The configurations (a) with  $n_k = 2$ , (c) and (d) with  $n_k = 4$  are acceptable by Cu in the chains, but Li can only accept the configuration (a). As the configuration (c) is absolutely dominant in fully oxygenated Y123, we consider the coordination (d) as well as other configurations with  $n_k > 4$  energetically unfavorable and their presence should be minimized. However, the configuration (d) is always present when Li substitutes Cu in the chains as shown in figure 4 (g). The concentration of this configuration can be minimized by one or two dimensional clustering of Li atoms (figure 4 (h) and (i)). Li atoms can cluster at temperatures, where both the mobility of the Li ions in the Y123 lattice and the oxygen diffusion into the bulk are sufficiently high. Temperatures above about 700 °C would be suitable for this process, so pre-annealing in pure oxygen at 800 °C during the standard oxygenation process can lead to Li clustering. During pre-annealing in Ar at 800 °C the Li clusters are

dissolved and Li is more homogeneously (randomly) distributed in the Y123 matrix, leading to a decrease of  $T_c$ .

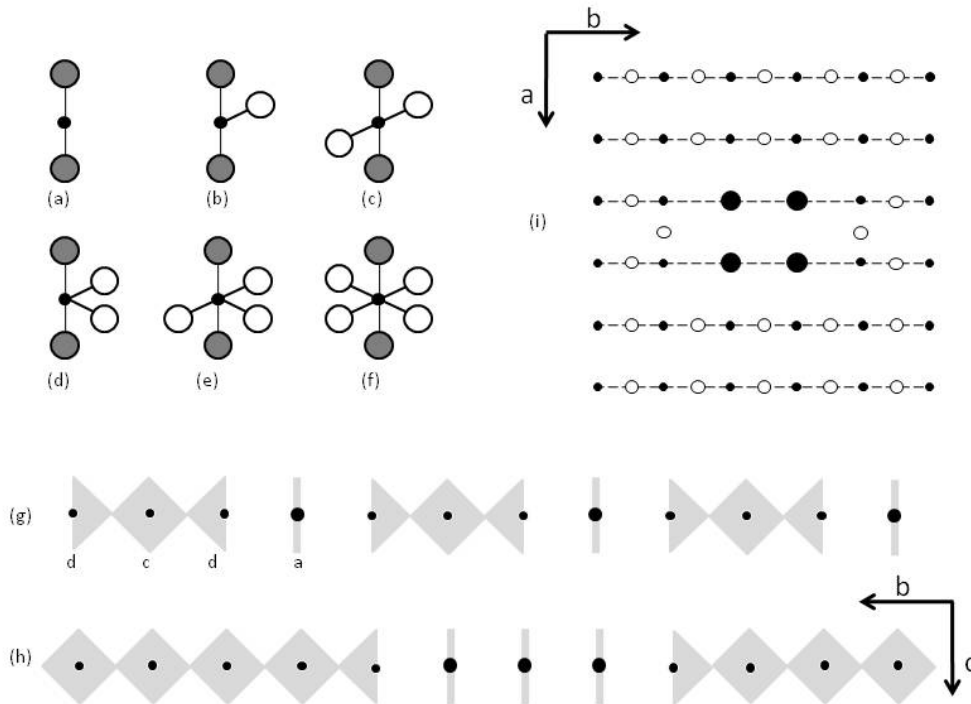


Figure 4. (a - f): Various oxygen configurations about the metal atom in the chains of the CuO plane. The solid circle indicates the metal atom. The open and full circles indicate in-plane and out-of-plane oxygen atoms, respectively.

(g - i): The concentration of (d) configurations is lower, when linear (h) or two dimensional (i) Li clusters are formed. The smaller solid circles represent the Cu atoms and the larger ones represent the Li atoms.

For both the Li and the Al dopants a peak effect in  $J_c$  appears at the lowest dopant concentration (Figures 2 (b) and 3 (b)). According to Ishii [15] the peak effect in RE123 melt processed samples with RE elements, which do not substitute Ba (for example Y and Dy), should be observed at a dopant concentration leading to a distance between randomly distributed dopant atoms in the  $\text{CuO}_2$  plane of 2 coherence lengths, which is about 6 nm. In our case this mean distance between randomly distributed substituent atoms is reached for  $x = 0.0013$ , when they substitute Cu in the CuO chains, and for  $x = 0.0026$ , when they substitute for Cu in the  $\text{CuO}_2$  planes. This doping level corresponds to our lowest concentration. Interesting are the changes caused by the post-growth heat treatments. An additional heat treatment of the samples with Al doping in argon at 800 °C for 1 hour shifted the appearance of the peak effect to the highest Al concentration,  $x = 0.05$ , which corresponds well with Al clustering. If we assume clustering of Al atoms and an effective mean distance between Al clusters of 6 nm, we expect about 20 Al atoms in an Al cluster. Pre-annealing in Ar also led to a more pronounced peak effect, which can be associated with the dissolution of Li clusters (formed during cooling of the bulk in air) leading to a random distribution of individual Li ions in the  $\text{CuO}_2$  plane and more effective pinning.

High pressure high temperature oxygenation preserved the peak effect caused by the dopants and had a significant effect on the absolute value of the critical current density, which was 2.5 – 3 times

higher than for the other treatments for both dopants. As was already shown [4], this  $J_c$  improvement is caused by the elimination of oxygenation cracks, which increases the effective sample cross section by up to 3 times [16].

## 5. Conclusions

Post-growth heat treatments revealed a different behavior of Li and Al doped TSMG YBCO bulk samples, which was associated with clustering and dissolution of clusters of the dopant atoms. The changes in critical temperature,  $T_c$ , and in critical current density were explained by clustering of Al atoms during annealing in low oxygen partial pressure atmosphere and by a random Al distribution after pre-annealing in oxygen. Lithium doping results in the opposite behavior being caused by clustering during annealing in oxygen and random distribution after annealing in argon. High pressure high temperature oxygenation preserved the peak effect in  $J_c$  caused by the dopants and had a significant effect on the absolute value of the critical current density, which was 2.5 – 3 times higher than for other treatments for both dopants.

## Acknowledgements

This work was performed within the frame of the project “Centre of Excellence of Advanced Materials with Nano- and Submicron- Structure”, and the project NFP26220220056 (ITMS 26220220041), supported by the Operational Program “Research and Development” financed through the European Regional Development Fund, by the VEGA project No.- 2/7052/27, the APVV projects No. 51-061505 and LPP-0334-06, the EU Marie Curie network NESPA, and by the Centre of Excellence of the Slovak Academy of Sciences NANOSMART.

## References

- [1] Shlyk L, Krabbes G, Diko P, Nenkov K, Fuchs G 2004 *J. Phys.: Conf. Ser.* **181** 1401
- [2] Y. Ishii, J. Shimoyama, Y. Tazaki, T. Nakashima, S. Horii, and K. Kishio, 2006 *Appl. Phys. Lett.* **89** 202514.
- [3] P. Diko, V. Antal, M. Kaňuchová, M. Šefčíková, J. Kováč, 2009 *Journal of Physics: Conference Series* **153** 012009.
- [4] P. Diko, X. Chaud, V. Antal, M. Kaňuchová, M. Šefčíková and J. Kováč, 2008 *Supercond. Sci. Technol.* **21** 11508.
- [5] Bean C P 1962 *Phys. Rev. Lett.* **8** 250.
- [6] P. Diko, M. Šefčíková, M. Kaňuchová, K. Zmorayova, 2008 *Materials Science and Engineering B* **151** 7–10.
- [7] Lacayo G, Koestner G, Herrmann R, 1992 *Physica C* **192** 207.
- [8] Renevier HP, Hodeau JL, Marezio M, Bessière M, Elkaïm E, Lefèbvre S, 1994 *Physica C*, **220** 143.
- [9] M. Nicolas-Francillona, F. Mauryb, M. Nanotc, R. Ollitrault-Fichetc 1999 *Solid State Communications* **109** 531.
- [10] B. Liu, X. Xy, R. Tao, Z. Xu, J. Shen, Q. Pu, G. Wang, Z. Ding 2004 *Physica C* **403** 313.
- [11] G. H. Kwei, K. C. Ott, E. J. Petterson 1992 *Physica C* **194** 307.
- [12] F. Maury, M. Nicolas-Francillon, I. Mirebeau, F. Bourée 2001 *Physica C* **353** 93.
- [13] R. D. Shannon, 1976 *Acta Cryst.* **A32** 751.
- [14] E. Takayama-Muromachi, 1990 *Physica C* **172** 199.
- [15] Y. Ishii, Y. Yamazaki, T. Nakashima, H. Ogino, J. Shimoyama, S. Horii, K. Kishio, 2008 *Materials Science and Engineering B* **151** 69.
- [16] M Eisterer, S Haindl, M Zehetmayer, R Gonzalez-Arrabal, H W Weber, D Litzkendorf, M Zeisberger, T Habisreuther, W Gawalek, L Shlyk and G Krabbes 2006 *Supercond. Sci. Technol.* **19** S530.